"Influence of ductile substrates and layer thickness on the spacing and topology of layer bound fault systems"

Mark T. Ireland[1*], Chris K. Morley[2] and Richard J. Davies[1]

[1]School of Natural and Environmental Sciences, Newcastle University, Drummond Building, Newcastle upon Tyne, NE1 7RU

[2]PTTEP, Enco, Soi 11, Vibhavadi Rangsit Road, Chatuchak, Bangkok, 10900, Thailand

**Corresponding author: mark.ireland@newcastle.ac.uk, https://orcid.org/0000-0001-9777-0447*

This manuscript has been submitted for publication in BASIN RESEARCH. The manuscript has not yet undergone peer review. Subsequent versions of this manuscript may have different content if accepted and the final version will be available via the "peer-reviewed Publication DOI" link.

Please feel free to contact the corresponding author directly to provide any constructive feedback

Influence of ductile substrates and layer thickness on the spacing and topology of layer bound fault systems

Mark T. Ireland[1*], Chris K. Morley[2] and Richard J. Davies[1]
[1]School of Natural and Environmental Sciences, Newcastle University, Drummond Building, Newcastle upon Tyne, NE1 7RU
[2]PTTEP, Enco, Soi 11, Vibhavadi Rangsit Road, Chatuchak, Bangkok, 10900, Thailand

**Corresponding author: mark.ireland@newcastle.ac.uk, https://orcid.org/0000-0001-9777-0447*
Co-author: chrismorely@gmail.com
Co-author: richard.davies@newcastle.ac.uk

DATA AVALIBILITY

The data that support the findings of this study are openly available from Geoscience Austrailia at https://www.ga.gov.au/nopims

FUNDING

Mark Ireland is part funded by ReFINE (www.refine.org.uk)

CONFLICT OF INTEREST

There are no conflicts of interest.

ABSTRACT

Polygonal fault systems are extraordinary features of many fine grained sedimentary succession and have been described from a significant number of deepwater sedimentary basins over the last two decades. Their formation represents an important mechanism by which fine grained sediments compact often resulting in a variety of complex patterns for which several controlling factors have been proposed. Here three-dimensional seismic data from the North West Shelf of Australia are used to interpret previously undescribed characteristic of a layer

bound fault systems where systematic horst and graben structures are the dominant structural style. Conjugate fault pairs which form the horsts and grabens frequently have a systematic spacing with graben bounding faults exhibiting a spacing of half that of the horst bounding faults. It is interpreted that this systematic spacing of fault pairs indicates the presence of a ductile layer at the base of the fault system. Furthermore, using topological analysis areas with different patterns and contrasting fault interactions and intersections, are used to show that the growth of layer bound faults may not be explained by a single model of growth. The regular spacing and style of faults described indicate that the growth of layer bound fault systems are strongly influenced by both layer thickness and the ductility of underlying sediments. The findings have implications for the genesis and growth of layer bound fault systems.

INTRODUCTION

Polygonal faults are a ubiquitous feature in many deepwater, sedimentary basins on Earth (Cartwright, 2007). Polygonal faults systems (sometimes termed layer-bound faults), are commonly found in fine grained sedimentary successions and comprise networks of normal faults with orientations that commonly form polygonal geometries on bedding planes (Lonergan et al., 1998). The bedding plane geometries of compaction fault systems may depart from these polygonal forms due to the influence of external stresses such as basin floor slope (Higgs and McClay, 1993), tectonic faults (Hansen et al., 2004) and influence of stratigraphic features (Ireland et al., 2011). They are an important class of fault because they typically deform fine grained, low permeability sediments that are commonly sealing sequences for fluids in sedimentary basins (Cartwright et al., 2007) and represent a mechanism for sediment dewatering and compaction. They have been one of the most debated and enigmatic geological structures discovered using 3D seismic data. The characteristics of complex fault networks and fault interactions is important for understanding how mechanical layers cause variations in the displacement characteristics and scaling relationships of faults (Peacock, 2002).

Over the past two decades the increasing coverage, resolution and availability of three-dimensional (3D) seismic reflection data from sedimentary basins across the world has led to the widespread recognition of polygonal fault systems and numerous variations in their geometries (e.g. Morgan et al., 2015;Ghalayini et al., 2017). Increasingly analysis has shifted from qualitative descriptions to quantified structural analysis, including, but not limited to throw and displacement, orientation and topological analysis (e.g. Wrona et al., 2017;Morley and Binazirnejad, 2020). Here, observations and interpretations from 3D seismic data from the North West Shelf, Australia are used to describe the spacing and topology of layer bound fault systems, and the implications for their genesis and growth examined.

LAYER-BOUND FAULT SYSTEMS

The origin of polygonal fault systems have received a wide variety of interpretations but are generally accepted to be the result of volumetric reduction, with bed-parallel compaction, which complements the heaves on the faults, in addition to vertical compaction (Cartwright and Lonergan, 1996). Laboratory measurements (Bishop et al., 1971) and field data (Goulty and Swarbrick, 2005) suggest that low coefficients of friction on fault surfaces may be an important factor that allows polygonal fault systems to develop (Goulty and Swarbrick, 2005;Goulty, 2008). Once faults have nucleated in the fine-grained host sediment, they can continue to grow with increasing overburden stress under laterally confined conditions, provided that the coefficient of residual friction on the fault surfaces is sufficiently low (Goulty, 2008). Layer-bound faults have been identified in the siliceous sediments across the Australian Margin (Seebeck et al., 2015;Alrefaee et al., 2018). Geometric and topological analysis of fault systems is important to investigating their evolution (e.g. Duffy et al., 2017) and the role that, for example, lithology variations and factors such as depositional and stratigraphic setting, gravitational instability, post faulting compaction have.

Fault systems are commonly characterized by the geometry of faults (e.g.Barnett et al., 1987) and the characteristics of fault networks (e.g. Bour and Davy, 1998) which includes fault spacing (Barnett et al., 1987;Soliva and Benedicto, 2005) and connectivity (Sanderson and Nixon, 2015). The mechanics which control and influence fault spacing in normal fault populations is applicable to both polygonal or layer bound fault systems, as well as other fault populations which are confined to discrete mechanical layers (Benedicto et al., 2003). Regular patterns of fault spacing can occur at different scales and is often attributed to the thickness of the mechanical layer (Soliva et al., 2006). The role played by layer thickness in controlling vertically restricted faults systems has been linked to the variations in mechanical strength in layered sequences (e.g. Benedicto et al., 2003). There are have been numerous analogue studies which investigate the role of basal detachments (Axen, 1988) and deformable substrates (Li and

Mitra, 2017), in extensional regimes. These studies have highlighted the role that rheological differences can have in different patterns of normal faults with both hard and soft linkages (Bahroudi et al., 2003). Recently the application of topological analysis in fault and fracture networks has been used to provide quantitative descriptions of fracture networks, and used the geometric differences to help to understand their genesis (Morley and Nixon, 2016). The topology of fault and fracture networks can be characterized by branches and nodes (Manzocchi, 2002). There are three types of node, isolated tips (I); crossing fractures (X); and abutments or splays (Y-nodes or T-nodes). Commonly fractures terminate against (or abut) pre-existing fractures, producing many Y-nodes. Morley and Binazirnejad (2020) described the detailed topology of polygonal fault sets to investigate variations in connectivity and identified that the polygonal fault sets share similarities in node and branch topology with complex tectonic fault patterns in rifts.

DATABASE AND METHODOLOGY.

The 3D seismic survey was acquired in 2002 on the Exmouth Plateau on the North West Shelf of Australia, provided by Geoscience Australia was interpreted (Fig. 1a). The data are post-stack time migrated with a bin spacing of 12.5 × 12.5 m and the vertical resolution is ~ 10 m. The data are zero-phased, with SEG reversed polarity (SEG, 2019), where a positive reflection coefficient with a central peak is normally plotted as a black on a variable area or variable density display representing an increase in acoustic impedance, and a black-red-black reflection. The interpreted seismic horizons were tied to the nearby exploration well, Moyet-1, which is also used to describe the lithology of the interval studied (Fig. 1). A series of horizons from stratigraphic reflections were interpreted and subsequently the reflection geometrical properties (e.g. Chopra and Marfurt, 2012) and seismic attributes (Bacon et al., 2007) were used to describe the planform geometries of the observed polygonal faults systems. Given the large number of polygonal faults within a single system this study used both manual and automated fault interpretation methods. To interpret fault orientation, we extract lines from horizon attributes. The variance attribute uses a window analysis across the seismic volume to calculate the degree of trace to trace similarity along the selected dip within the defined 3D window, which can be interpreted as lateral changes in acoustic impedance (Barnes, 2016). Variance has been widely used (Chopra and Marfurt, 2008) in seismic interpretation studies of structural features. Using detailed interpretations of stratigraphic horizons allows for the planform geometries and intersections to be mapped out in detail. Detailed fault plane interpretations and horizon interpretations allows the geometries of faults and their displacements to be analysed. To analyse the spacing of faults a scan line approach was adopted (e.g. Soliva et al., 2006). Fault spacing was measured along 4 scan lines, 2 inlines (IL 3400 and 3500) and 2 crosslines (XL 4400 and 4600), each ~30 km long (Fig. 2). The spacing distance was measured on the T10 horizon between bounding faults of horsts, bounding faults of grabens, and bounding faults where they have the same dip direction. The T10 horizon was chosen because 1) the faults have b-type displacement depth-profiles (e.g. Wrona et al., 2017) and therefore exhibit displacement maxima located towards to the lower tip, 2) it is a continuous reflection which can be mapped with high confidence through the faulted interval, and 3) it exhibits the most structural complexity of any single level within the fault system. Fault topology was analysed by using 3 sample areas (Fig 2.). The NetworkGT Tools (Sanderson and Nixon, 2015;Nyberg et al., 2018) were used to analyse the topology of the polygonal fault system with mapped fault traces interpreted from seismic from horizon interpretations as the input. The NetworkGT tools are an open source toolbox for ArcGIS which can be used to sample, analyse and spatially map the geometric and topological attributes of two-dimensional fracture networks (Nyberg et al., 2018). The NetworkGT toolbox is used with ArcGIS (version 10.6), and specifically the branch and node tools, to analyse the topology of the layer bound fault system. The analysis characterizes the branches and nodes of the fracture network and the results are presented in the form of maps, rose diagrams and histograms. Following Sanderson and Nixon (2015) we used the number of connections per branch ($\boldsymbol{C_B}$) to provide a measure of connectivity of the faults systems, which is given by Eq 1.

$$\boldsymbol{C_B = (3N_Y + N_X)/N_B}$$

Equation 1

GEOLOGICAL SETTING

The Exmouth Plateau is, bounded by the continental shelf to the southeast, and the Argo, Gascoyne and Cuvier abyssal plains to the northeast, northwest and southwest, respectively (Longley et al., 2002). The Exmouth Plateau is part of the North Carnarvon Basin, which experienced several rifting events between the Late Carboniferous and Early Cretaceous, with seafloor spreading commencing in the Argo Abyssal Plain in the Late Jurassic and in the Gascoyne and Cuvier abyssal plains in the Early Cretaceous (Tindale et al., 1998; Longley et al., 2002). Changes in depositional style have been linked to regional tectonic processes on the Exmouth plateau where the stratigraphy records plate-scale geological events (Nugraha et al., 2019). The 3D seismic data is located on the Exmouth Plateau and to the west of the Kangeroo Syncline (see Fig. 1). The faulted interval comprises recent to Campanian age stratigraphy, which is constrained by the Moyet-1 well (Fig. 1b).

The recent to Pliocene (Delambre Fomration) interval extends down from the seafloor to the T40 sequence boundary, which is a prominent peak event in the area, tied to the nearby Moyet-1 well. The Miocene to Eocene (Bare to Upper Walcott Formations) is marked at the top by the T40 sequence boundary and the base is marked by the T27 horizon. The Eocene to Paleocene (Lower Walcott and Dockrel Formations) is marked at the top by the T27 horizon, and at the base by the T10 horizon. A description of the interval of interest is provided in the Moyet-1 well report (Woodside, 2011). The Dockrell Formation commonly comprises marine marls and clays, and the Walcott is typically comprising calcareous foraminiferal and clays. The Maastrichtian to Campanian (Mira and Withnell Formations) is marked at the top by the T10 horizon and the base at the K60 horizon. The top and base of the Campanian to Aptian (Toolonga Calcilutite and Haycock Marl) interval are the K60 and K40 markers respectively. The Miria Formation is commonly composed marine marl and the Withnell of calcareous clays. There are no samples or core over the faulted interval, however wireline log data indicate a marked increase in the gamma ray response at the T10 horizon. The primary interval of interest is the Miocene to Maastrichtian section which comprises a succession of dominantly fine-grained calcareous sediments

SEISMIC OBSERVATIONS AND INTERPRETATIONS

Faulted Interval

The primary interval of interest is between the Miocene to Maastrichtian section. The succession comprises dominantly fine-grained calcareous sediments and has a network of normal faults developed across the survey area throughout this interval. Individual faults may separate polygonal fault blocks of un-faulted sediment. Across much of the area the polygonal fault blocks are often bounded not by a single fault, but by conjugate, graben forming pairs (see Fig 3 and 4). The faults predominantly form a single tiered network, although there are occasional faults which are antithetic to large faults and which only offset the upper part of the interval (see Fig. 3). There are obvious variations in the planform geometry of the faults from the T10 time structure maps, and the variance attribute maps (Fig. 5). Thickness variations are apparent across the area, with measurable differences in the gross interval thickness of the T10 to T27 intervals, as well as subtle thickness variations across individual horst and graben fault blocks. From the T10 to K60 horizon, beneath the downthrown grabens the interval is clearly thinner than beneath the adjacent fault blocks (Fig. 6). The conjugate graben pairs generally have lower tips which converge or intersection near the middle of the Maastrichtian to Campanian section (Mira and Withnell Formations) (Fig 3).

Fault Geometry and Spacing

The geometries of individual faults forming the fault network varies from planar to listric. In general faults with a greater vertical extent (and typically with a greater displacement) may have a listric geometry, while faults with a limited vertical extent and smaller displacements are closer to planar. Faults with their lower tips below the T10 stratigraphic horizon are more commonly listric, whereas those restricted to above are more planar. Fig. 3 shows XL3500 with an interpretation of horsts, grabens and fault blocks bounded by the same dip direction faults. This interpretation is based on the geometry at the T10 sequence boundary, which is located towards the lower tips of the faults in the system. Along this section there are 18 conjugate faults which form horsts, 17 which form grabens and 23 segments with the same dip direction. At the base of the faulted interval, the normal faults which define horsts and grabens rarely intersect or displace adjacent faults, which could be interpreted as indicating that fault initiation and propagation is contemporaneous across the study area. Across all 4 scanlines a total 264 fault spacings and segment types were measured with 29% forming conjugate sets which are horsts, and 28% being conjugate sets which are grabens. The average spacing of conjugate graben forming faults is 236m compared with 543m for conjugate horst forming faults. Fig. 7 shows the distribution of fault spacing for the different fault segments types and shows overall a logarithmic distribution of fault spacing. The conjugate horst pairs exhibit a log-normal distribution (p-value = 0.009) and 64% of this population have a spacing greater than the average for the whole sample population. The conjugate pairs that form graben pairs fit a log-normal distribution (p-value = 0.145) and of these faults 91% have a spacing less than the average for whole sample population. Where a fault block is bound by the same dip direction faults, the segments broadly fit a log-normal distribution (p-value <0.005). Of these faults 25% have a spacing greater than the average of the whole population. The standard deviation for fault spacing of grabens is 94m, compared with 227m for faults blocks bounded by the same dip faults and 340m for horsts. The pronounced differences in fault spacing between horst and graben conjugates suggest that fault spacing, and dip direction, is controlled not by random nucleation and growth, but a systematic control at the kilometre scale.

Fault Topology and Orientations

The topological analysis which is shown in Fig. 8a-c show the difference in the combinations of branch and node types in each sampled area. For Area A, 45.8% of the branches are C-I, 25.1 % are I-I and 29.1% are C-C. For Area B, 49.5% of the branches are C-I, 26.7 % are I-I and 23.8% are C-C. For Area C, 30.5% of the branches are C-I, 67.3% are I-I and 2.2% are C-C. Area A and B exhibit a similar topology and are the most complex, with less than a third of the faults in both areas being isolated. Faults in areas A and B commonly exhibit intersecting faults. In contrast Area C is, topologically, much simpler, with almost two thirds of the sampled faults being completely isolated. When looking at the proportion of nodes in each sample area, Y type nodes account for 4 and 5 times the proportion of nodes in Areas A and B compared with Area C. Over 90% of nodes in Area C are I type, as is expected for a fault system dominated by isolated faults. Due to the high proportion of isolated branches the fault system sampled in Area C can be interpreted as having a low level of connectivity. This is in contrast to Areas A and B. Using Eq. 1 to determine the average number of connections per branch, Area A is 0.91 and Area B is 0.90, while Area C is 0.29.

In map view the overall geometry of the fault system is polygonal, however there are clearly identifiable variations across the survey. For Area A the map patterns show the polygonal fault systems is dominated by two preferred orientations 0° and 90°, orthogonal to one another which are 10% and 11% of the total sample (Fig. 8d). For Area B the map patterns show the polygonal fault systems broadly exhibit an even distribution of strikes, with faults orientation at 170° having ~9% of all fault strikes, with two strongly preferred orientations at 0° and 90°, orthogonal to one another (Fig. 8e). For Area C the map pattern exhibits a rectilinear geometry and is dominated by faults oriented at 30° (~18% of all fault strikes) and 120° (~7% of all fault strings; Fig. 8f). In areas where deeper tectonic faults are present, the polygonal fault system is strongly influenced by the orientation of these faults. Over 90% of the polygonal faults within 1km horizontal distance of the trace of the underlying larger tectonic faults show the same orientation to as the tectonic faults. It is worth noting that as well as the relationship of faults strike orientation to the underlying features, there also appears to be a dominance of narrow graben conjugate pairs above these tectonic features (Fig. 5b and Fig 6a)

Fault Length

Histograms for fault length are shown in Fig. 9a-c for Areas A, B and C. All three sample areas have a right skewed distribution, with sample populations of all branch types dominated by a higher proportion of shorter fault segments. In Area A, the mean length of I-I faults is 500m, C-I is 345m and C-C is 345m (Fig. 8a). In Area B, the mean length of I-I faults is 372m, C-I is 344m and C-C is 282m (Fig. 8b). In Area C, the mean length of I-I faults is 305m, C-I is 233m and C-C is 158 (Fig. 8c). In Area A and B the T10 to T27 time thickness is dominantly between 220 and 280ms, with Area A being on average thicker than Area B (Fig. 6). In Area C the time thickness is dominantly 180 to 220ms. For all branch types the mean fault length is greater where the layer thickness is greater. Across all areas the mean and median length of I-I branches is greater than C-C branches.

DISCUSSION

Fault Spacing and Orientation

The polygonal fault system interpreted in this study show a system of normal faults dominated by conjugate pure shear (e.g.Stewart and Argent, 2000). The systematic variation in faults spacing and dip direction suggest that fault growth is not random but related to a systematic control at the kilometre scale. In Areas A and B where the T10 to T27 is thicker, the fault spacing is greater than Area C which suggests that final, or late stage spacing of faults in layer-bound fault systems are could exhibit close to a linear dependency to layer thickness (e.g. Soliva et al., 2006). Though we do not have another dataset for comparison, qualitative assessment of other published polygonal fault systems indicate that this is not common. The analysis from Soliva et al. (2006) while observing similar horst – graben configurations and with an overall normal distribution, these accounted for only a very small proportion of the whole population. Here the analysis indicates that horst and graben fault blocks account for up to ~50% of the total population. The models of models of Victor and Moretti (2006) also exhibited similar horst – graben fault geometries. Vétel et al. (2005) suggested that the systematic spacing of horst–graben pairs and the exponential spacing distributions in the Turkana Rift indicate the presence of a dominating km-scale structural control complicated by randomly distributed smaller faults. Since layer bound fault systems are typically restricted to a stratigraphic interval, the mechanical thickness of the interval likely exhibits an important control on the spacing. Typically a single fault cannot accommodate the progressive increase of strain and as a result further faults are required, which has been shown in both outcrop and analogue models of extensional faulting in layered systems (Bahroudi et al., 2003;Benedicto et al., 2003;Soliva et al., 2005). In the fault system described here, it is postulated that the dominance of large unfaulted horst blocks surrounded by narrow grabens, indicates that the Miocene to Maastrichtian interval has accommodated the horizontal shortening required by the volume loss due to compaction but significantly, without reaching saturation with respect to fault density (e.g. Ackermann et al., 2001). The style of deformation observed is consistent with that of a frictional overburden uniformly extended above a frictional detachment, as described in analogue models by Bahroudi et al. (2003). Their analogue models identified that grabens were wider above a ductile detachment than above frictional detachments. The properties of substrates are discussed later. The geometry of the areas dominated by conjugate faults is akin to the geometry of faults identified in gravity spreading systems (e.g. Schultz-Ela, 2001) which would suggest that the lower most part of the Maastrichtian to Campanian (Mira and Withnell Formations) interval marks a transition from brittle to ductile behaviour**.** It is interpreted that during early fault growth that polygonal rafts formed separated by narrow graben structures. For the conjugate pairs of faults forming horsts and grabens, it is likely the faults formed coevally and intersect at their tips to form a polygonal pattern. It is reasonable to interpret, that, given that the network of polygonal grabens in Areas A and B has no preferred orientation, that the apparent extension, and ultimately strain also has no preferred orientation.

Polygonal Fault Development

The topological analysis and the variations in fault orientation indicate, that despite the polygonal fault system being pervasive across the survey area in the T40 to K60 interval, that the development of the fault system, and the interaction and subsequent intersection between neighbouring faults varies considerably. In Area C the dominance of a single orientation and of I-I branches indicate there is significant variation in the stress field from Areas A and B which are exhibit a more typical polygonal pattern and proportionally more intersections. Morley and Binazirnejad (2020) described that topology offers a way to describe polygonal fault network complexity, and when combined with other observations may also help discriminate between the origins of different complex fault types. While the analysis presented here does not definitively confirm that Areas A, B and C have a different genesis, it is difficult to reconcile that the contrasting topologies, orientations and geometries interpreted across the fault system can be explained by a single evolution. Area A, which shows no preferred orientation, and can be considered topologically the most complex due to the high proportion of C-I and C-C branches also has a high proportion of conjugate pairs forming horsts and graben. This area represents the systematic development of a polygonal fault system with very limited external forcing, such as pre-existing structures (e.g. Hansen et al., 2004) and stratigraphic dip (e.g. Ireland et al., 2011) or the influence of regional stresses. In Area C, where the same T40 to K60 is faulted, there is an absence of conjugate pairs, a dominant orientation, and a high proportion of I-I branches. This area has most likely been influenced by stratigraphic dip and regional stress. As would be expected, where a single orientation of fault dominates the likelihood of C-C branches and crossing fractures (X); and abutments or splays (Y-nodes or T-nodes) decreases. The systematic variation in branch type length may also reveal details of the genesis and growth of the fault system. The mean fault length of I-I branches is always greater than C-C branches, and this could indicate that C-C fault branches are the last fault segments to grow and their trace length is restricted by already. As shown by Soliva et al. (2006) the stress drop around the faults is likely linearly related to the thickness of the layer and indicates that layer thickness may also play a role in controlling the extent of the stress reduction and therefore fault spacing within the system.

The analysis here indicates that while clearly the orientation of faults within a layer bound system are influenced by regional or tectonic stresses, the growth and evolution of the systems, and the likelihood of fault – fault interactions is too. The analysis showed that the average number of connections per branch is three times higher in areas with no preferred fault orientation (polygonal patterns) compared with and areas with a single dominant orientation. In fault systems where there is a single dominant orientation directional permeability may develop orthogonal to fault slip direction (Sibson, 1996). In areas with conjugate faults and more frequent X, Y or T nodes, the extensional-shear fractures may develop in pipe like conduits and act as preferential pathways for cross stratal fluid flow (Sibson, 2000). Cartwright et al. (2007) identify that polygonal fault systems, and more generally faults embedded in a sealing sequence, are important geological features which enable seal bypass. The connectivity of a polygonal fault system is likely important in understanding the potential for cross stratal fluid flow. Observed variations in the topology of layer bound fault systems may strongly influence fluid flow and may be expressed in the resulting patterns of fluid expulsion features through otherwise low permeability (Waghorn et al., 2018)

Pure Shear and Detachment

In analogue models with a mobile substrate or detachment at the base (akin to evaporites or shales), the formation of polygonal fault patterns has been attributed to brittle 3D extension imposed by lateral flow of the ductile substrate (Victor and Moretti, 2006). The sequence of sediments here is dominated by the fine grained calcareous and clay rich formations. Ductile deformation of clay-rich sediments has been observed in different geological settings and less frequently ductile deformation within these intervals has been indicated by S–C-foliations reported in core (Takizawa and Ogawa, 1999). In the models of Victor and Moretti (2006) normal faults-bounding polygonal fault blocks appear regularly spaced in all of the experiments, and localize on top of silicone ridges rising from the basal silicone layer. Similar structures geometrically have been attributed to the rise of salt diapirs or shale diapirs are described by various authors (Vendeville and Jackson, 1992;Cohen and McClay, 1996;Morley et al., 1998;Rowan et al., 1999). Though the 3D seismic data here do not provide any clearly discernible ductile deformation features in the interval below the T10 stratigraphic horizon, the pattern of deformation observed in the layer bound faults form areas A and B would indicate that this is extremely likely. Though there is limited control on the lithology and mechanical properties of the faulted interval, in general the Dockrell and Walcott Formations are described as having a greater proportion of calcareous and biogenic components, which the underlying Mira and Withnell Formations may have a greater clay component. During shallow burial the lithologies that are commonly affected by layer bound fault systems are likely capable of deforming in a ductile manner. The contrast between brittle or ductile deformation in low-temperature settings is regarded as being temperature independent (Rutter and Hadizadeh, 1991). Argillaceous sediments may exhibit transitional brittle–ductile behaviour which favour shear failure under high differential stresses and ductile shear under small differential stresses (Dehandschutter et al., 2005). Variations and contrasts in the rheology and mechanical properties of fine grained sequences, as well as their stress state sequence, may favour particular layers behaving in a more ductile manner and therefore acting as a mobile substrate or detachment (e.g. Ireland et al., 2011). The presence of listric faults in the system, may qualitatively indicate that the faults initiate in the layer exhibiting more brittle behavior and subsequently flatten down towards ductile substrate after further extension (e.g. Ellis and McClay, 1988). The interpretation that the listric geometry is the result of fault growth and detachment is favored, as it is consistent with the previous explanation of fault spacing. Though subsequent compaction of the already faulted interval cannot be ruled out (e.g. Neagu et al., 2010), given that the observed changes in fault plane flattening are not systematic or pervasive through the system, it is not considered a dominant control on the observed fault geometries.

CONCLUSIONS

This is the first time that systematic variations in the spacing and topology of layer-bound faults have been described. The regular spacing of faults suggests, that their growth is strongly influenced by both layer thickness and the ductility of underlying sediments which is consistent with normal faults in other vertically restricted systems,. The findings have implications for the mechanics of not only polygonal faults, but vertically restricted normal faults more broadly. Variations in the topology and geometry of layer bound fault systems may strongly influence fluid flow through otherwise low permeability sequences and is therefore important for understanding the sealing integrity of overburden sequences for the geological storage of carbon dioxide and hydrogen. The observations and characteristics of the fault systems described provide valuable insights for the modelling and prediction of sub-seismic faults and fractures. To date, existing studies have looked to ascribe a single genesis to explain the formation of layer bound or polygonal faults systems (see Cartwright et al., 2003;Goulty, 2008). However, the observations and analysis here demonstrate that the fault spacing, and topology are inherently linked to the local geological setting (e.g. Davies et al., 2009), suggesting that the growth and potentially the genesis, of layer bound fault systems may be location specific. Further investigations from a wider sample of fault systems in different sedimentary basis is needed to examine whether the spacing, geometry and topology of layer bound fault systems can help distinguish faults with different genesis and growth histories.

ACKNOWLEDGMENTS

Seismic data were provided by Geoscience Australia and used under Open Access license. Data were interpreted using Schlumberger Petrel software provided under academic license. The interpretations of the stratigraphic horizons used in this study are provided in x,y,z ascii format and are available online. Early on this work benefitted from discussions with Chris Jackson and Craig Magee.

REFERENCES

Ackermann, R.V., Schlische, R.W., and Withjack, M.O. (2001). The geometric and statistical evolution of normal fault systems: an experimental study of the effects of mechanical layer thickness on scaling laws. *Journal of Structural Geology* 23**,** 1803-1819.

Alrefaee, H.A., Ghosh, S., and Abdel-Fattah, M.I. (2018). 3D seismic characterization of the polygonal fault systems and its impact on fluid flow migration: An example from the Northern Carnarvon Basin, Australia. *Journal of Petroleum Science and Engineering* 167**,** 120-130.

Axen, G.J. (1988). The geometry of planar domino-style normal faults above a dipping basal detachment. *Journal of Structural Geology* 10**,** 405-411.

Bacon, M., Simm, R., and Redshaw, T. (2007). *3-D seismic interpretation.* Cambridge University Press.

Bahroudi, A., Koyi, H.A., and Talbot, C.J. (2003). Effect of ductile and frictional décollements on style of extension. *Journal of Structural Geology* 25**,** 1401-1423.

Barnes, A.E. (2016). *Handbook of poststack seismic attributes.* Society of Exploration Geophysicists.

Barnett, J.A., Mortimer, J., Rippon, J.H., Walsh, J.J., and Watterson, J. (1987). Displacement geometry in the volume containing a single normal fault. *AAPG Bulletin* 71**,** 925-937.

Benedicto, A., Schultz, R.A., and Soliva, R. (2003). Layer thickness and the shape of faults. *Geophysical Research Letters* 30**,** n/a-n/a.

Bishop, A.W., Green, G., Garga, V.K., Andresen, A., and Brown, J. (1971). A new ring shear apparatus and its application to the measurement of residual strength. *Geotechnique* 21**,** 273-328.

Bour, O., and Davy, P. (1998). On the connectivity of three-dimensional fault networks. *Water Resources Research* 34**,** 2611-2622.

Cartwright, J. (2007). The impact of 3D seismic data on the understanding of compaction, fluid flow and diagenesis in sedimentary basins. *Journal of the Geological Society* 164**,** 881-893.
Cartwright, J., Huuse, M., and Aplin, A. (2007). Seal bypass systems. *AAPG Bulletin* 91**,** 1141-1166.
Cartwright, J., James, D., and Bolton, A. (2003). The genesis of polygonal fault systems: a review. *Geological Society, London, Special Publications* 216**,** 223-243.
Cartwright, J.A., and Lonergan, L. (1996). Volumetric contraction during the compaction of mudrocks: A mechanism for the development of regional-scale polygonal fault systems. *Basin Research* 8**,** 183-193.
Chopra, S., and Marfurt, K. (2012). Seismic attribute expression of differential compaction. *CSEG Recorder* 37.
Chopra, S., and Marfurt, K.J. (2008). Emerging and future trends in seismic attributes. *The Leading Edge* 27**,** 298-318.
Cohen, H.A., and Mcclay, K. (1996). Sedimentation and shale tectonics of the northwestern Niger Delta front. *Marine and Petroleum Geology* 13**,** 313-328.
Davies, R.J., Ireland, M.T., and Cartwright, J.A. (2009). Differential compaction due to the irregular topology of a diagenetic reaction boundary: a new mechanism for the formation of polygonal faults. *Basin Research* 21**,** 354-359.
Dehandschutter, B., Vandycke, S., Sintubin, M., Vandenberghe, N., and Wouters, L. (2005). Brittle fractures and ductile shear bands in argillaceous sediments: inferences from Oligocene Boom Clay (Belgium). *Journal of Structural Geology* 27**,** 1095-1112.
Duffy, O.B., Nixon, C.W., Bell, R.E., Jackson, C.a.-L., Gawthorpe, R.L., Sanderson, D.J., and Whipp, P.S. (2017). The topology of evolving rift fault networks: Single-phase vs multi-phase rifts. *Journal of Structural Geology* 96**,** 192-202.
Ellis, P., and Mcclay, K. (1988). Listric extensional fault systems-results of analogue model experiments. *Basin Research* 1**,** 55-70.
Ghalayini, R., Homberg, C., Daniel, J.M., and Nader, F.H. (2017). Growth of layer-bound normal faults under a regional anisotropic stress field. *Geological Society, London, Special Publications* 439**,** 57-78.
Goulty, N.R. (2008). Geomechanics of polygonal fault systems: a review. *Petroleum Geoscience* 14**,** 389-397.
Goulty, N.R., and Swarbrick, R.E. (2005). Development of polygonal fault systems: a test of hypotheses. *Journal of the Geological Society* 162**,** 587-590.
Hansen, D.M., Shimeld, J.W., Williamson, M.A., and Lykke-Andersen, H. (2004). Development of a major polygonal fault system in Upper Cretaceous chalk and Cenozoic mudrocks of the Sable Subbasin, Canadian Atlantic margin. *Marine and Petroleum Geology* 21**,** 1205-1219.
Higgs, W., and Mcclay, K. (1993). Analogue sandbox modelling of Miocene extensional faulting in the Outer Moray Firth. *Geological Society, London, Special Publications* 71**,** 141-162.
Ireland, M.T., Goulty, N.R., and Davies, R.J. (2011). Influence of stratigraphic setting and simple shear on layer-bound compaction faults offshore Mauritania. *Journal of Structural Geology* 33**,** 487-499.
Li, J., and Mitra, S. (2017). Geometry and evolution of fold-thrust structures at the boundaries between frictional and ductile detachments. *Marine and Petroleum Geology* 85**,** 16-34.

Lonergan, L., Cartwright, J., and Jolly, R. (1998). The geometry of polygonal fault systems in Tertiary mudrocks of the North Sea. *Journal of Structural Geology* 20**,** 529-548.
Manzocchi, T. (2002). The connectivity of two-dimensional networks of spatially correlated fractures. *Water Resources Research* 38**,** 1-1-1-20.
Morgan, D.A., Cartwright, J.A., and Imbert, P. (2015). Perturbation of polygonal fault propagation by buried pockmarks and the implications for the development of polygonal fault systems. *Marine and Petroleum Geology* 65**,** 157-171.
Morley, C.K., and Binazirnejad, H. (2020). Investigating polygonal fault topological variability: Structural causes vs image resolution. *Journal of Structural Geology* 130**,** 103930.
Morley, C.K., Crevello, P., and Ahmad, Z.H. (1998). Shale tectonics and deformation associated with active diapirism: the Jerudong Anticline, Brunei Darussalam. *Journal of the Geological Society* 155**,** 475-490.
Morley, C.K., and Nixon, C.W. (2016). Topological characteristics of simple and complex normal fault networks. *Journal of Structural Geology* 84**,** 68-84.
Neagu, R.C., Cartwright, J., and Davies, R. (2010). Measurement of diagenetic compaction strain from quantitative analysis of fault plane dip. *Journal of Structural Geology* 32**,** 641-655.
Nugraha, H.D., Jackson, C.a.-L., Johnson, H.D., Hodgson, D.M., and Reeve, M.T. (2019). Tectonic and oceanographic process interactions archived in Late Cretaceous to Present deep-marine stratigraphy on the Exmouth Plateau, offshore NW Australia. *Basin Research* 31**,** 405-430.
Nyberg, B., Nixon, C.W., and Sanderson, D.J. (2018). NetworkGT: A GIS tool for geometric and topological analysis of two-dimensional fracture networks. *Geosphere* 14**,** 1618-1634.
Peacock, D.C.P. (2002). Propagation, interaction and linkage in normal fault systems. *Earth-Science Reviews* 58**,** 121-142.
Rowan, M.G., Jackson, M.P., and Trudgill, B.D. (1999). Salt-related fault families and fault welds in the northern Gulf of Mexico. *AAPG bulletin* 83**,** 1454-1484.
Rutter, E., and Hadizadeh, J. (1991). On the influence of porosity on the low-temperature brittle—ductile transition in siliciclastic rocks. *Journal of Structural Geology* 13**,** 609-614.
Sanderson, D.J., and Nixon, C.W. (2015). The use of topology in fracture network characterization. *Journal of Structural Geology* 72**,** 55-66.
Schultz-Ela, D.D. (2001). Excursus on gravity gliding and gravity spreading. *Journal of Structural Geology* 23**,** 725-731.
Seebeck, H., Tenthorey, E., Consoli, C., and Nicol, A. (2015). Polygonal faulting and seal integrity in the Bonaparte Basin, Australia. *Marine and Petroleum Geology* 60**,** 120-135.
Seg (2019). *Dictionary:Polarity standard* [Online]. SEG. Available: https://wiki.seg.org/wiki/Dictionary:Polarity_standard [Accessed 20/10/2020].
Sibson, R.H. (1996). Structural permeability of fluid-driven fault-fracture meshes. *Journal of Structural Geology* 18**,** 1031-1042.
Sibson, R.H. (2000). Fluid involvement in normal faulting. *Journal of Geodynamics* 29**,** 469-499.
Soliva, R., and Benedicto, A. (2005). Geometry, scaling relations and spacing of vertically restricted normal faults. *Journal of Structural Geology* 27**,** 317-325.
Soliva, R., Benedicto, A., and Maerten, L. (2006). Spacing and linkage of confined normal faults: Importance of mechanical thickness. *Journal of Geophysical Research* 111.

Soliva, R., Schultz, R.A., and Benedicto, A. (2005). Three-dimensional displacement-length scaling and maximum dimension of normal faults in layered rocks. *Geophysical Research Letters* 32.

Stewart, S., and Argent, J. (2000). Relationship between polarity of extensional fault arrays and presence of detachments. *Journal of Structural Geology* 22**,** 693-711.

Vendeville, B.C., and Jackson, M.P. (1992). The rise of diapirs during thin-skinned extension. *Marine and Petroleum Geology* 9**,** 331-354.

Vétel, W., Le Gall, B., and Walsh, J.J. (2005). Geometry and growth of an inner rift fault pattern: the Kino Sogo Fault Belt, Turkana Rift (North Kenya). *Journal of Structural Geology* 27**,** 2204-2222.

Victor, P., and Moretti, I. (2006). Polygonal fault systems and channel boudinage: 3D analysis of multidirectional extension in analogue sandbox experiments. *Marine and Petroleum Geology* 23**,** 777-789.

Waghorn, K.A., Pecher, I., Strachan, L.J., Crutchley, G., Bialas, J., Coffin, R., Davy, B., Koch, S., Kroeger, K.F., and Papenberg, C. (2018). Paleo-fluid expulsion and contouritic drift formation on the Chatham Rise, New Zealand. *Basin Research* 30**,** 5-19.

Woodside (2011). "Moyet-1 Final Well Completion Report".).

Wrona, T., Magee, C., Jackson, C.A., Huuse, M., and Taylor, K.G. (2017). Kinematics of polygonal fault systems: observations from the northern North Sea. *Frontiers in Earth Science* 5**,** 101.

FIGURES

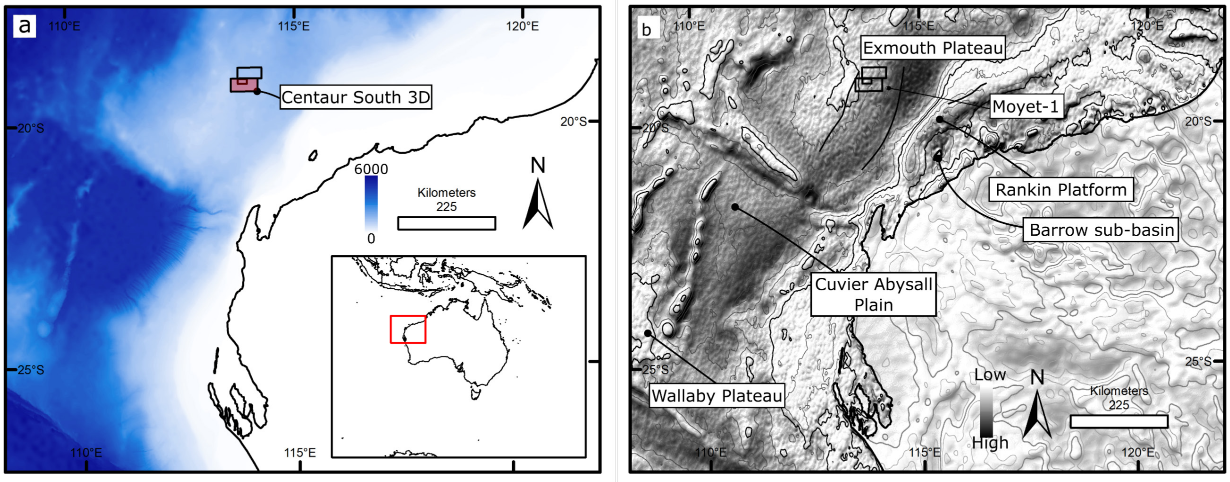

Fig. 1. Location map showing a) the location of 3D seismic survey in this study with the bathymetry of the Australian continental margin, red area denotes location of Fig 2 and b) bouguer gravity map across the same area, with some of the main basins and features of the margin indicated.

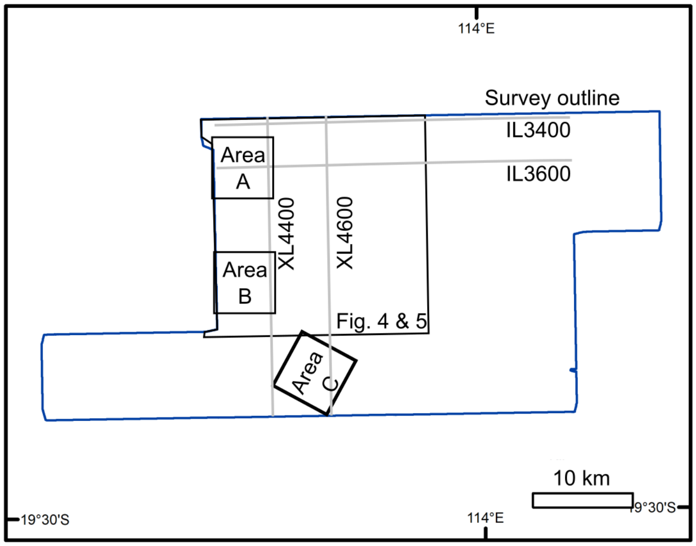

Fig 2. Map showing the location key seismic lines and zoomed in maps presented.

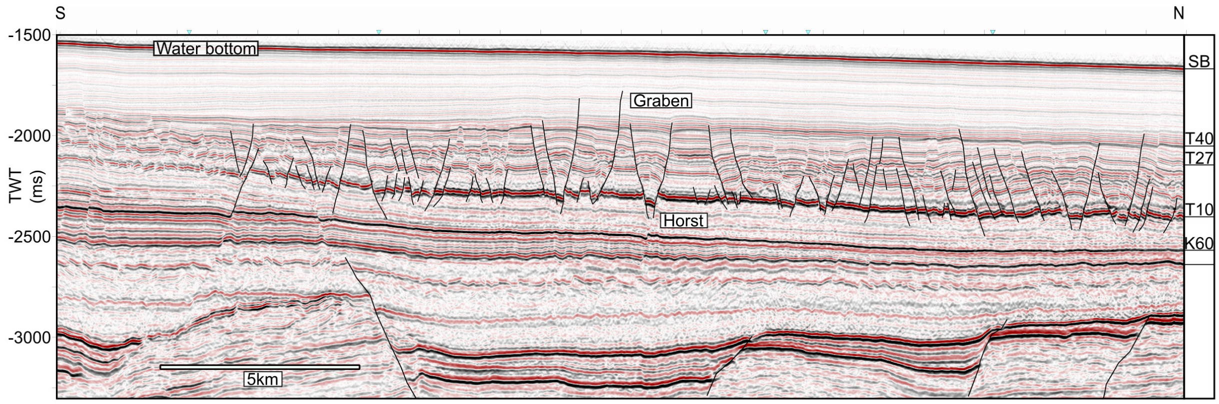

Fig. 3. Seismic profile through polygonal fault system with the key stratigraphic markers shown. The influence of underlying Campanian and older structures on the polygonal fault systems between T40 and K60 is described in the text.

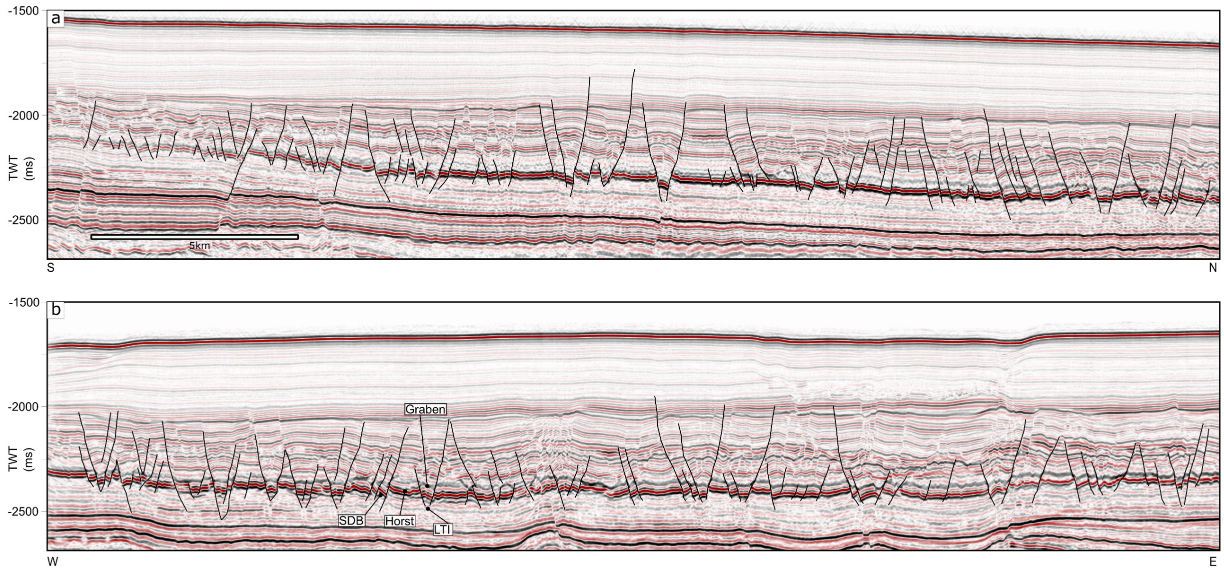

Fig. 4. Crossline 4400 (a) and Inline 3400 (b) seismic sections, showing the variation in fault geometry and the dominance of horst and graben conjugate pairs in the polygonal fault system. See Fig. 2 for location.

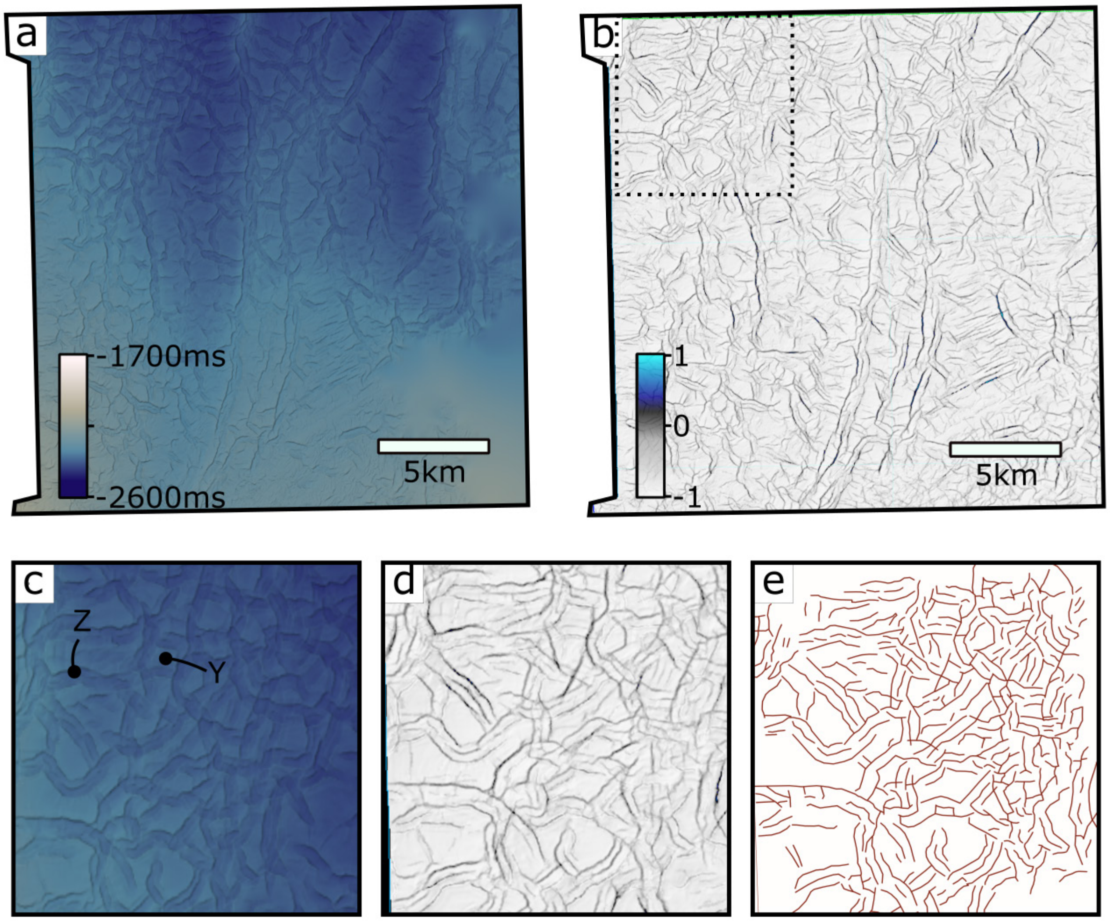

Fig. 5. Example of the horizon attributes and fault interpretation. (a) time structure map of T10, (b), ANT track seismic attribute map of the T10 and (c) zoom of time structure map, with Z indicating the position of a narrow graben and Y indicating the position of polygonal horst surrounded by a network of narrow grabens. (d) zoom of ANT track seismic attribute and (e) is an example trace of faults which are used for topological analysis. See Fig. 2 for location of (a) and (b). The interpreted horizon surfaces are available to download from the Data Repository at [INSERT WHEN ACCEPTED].

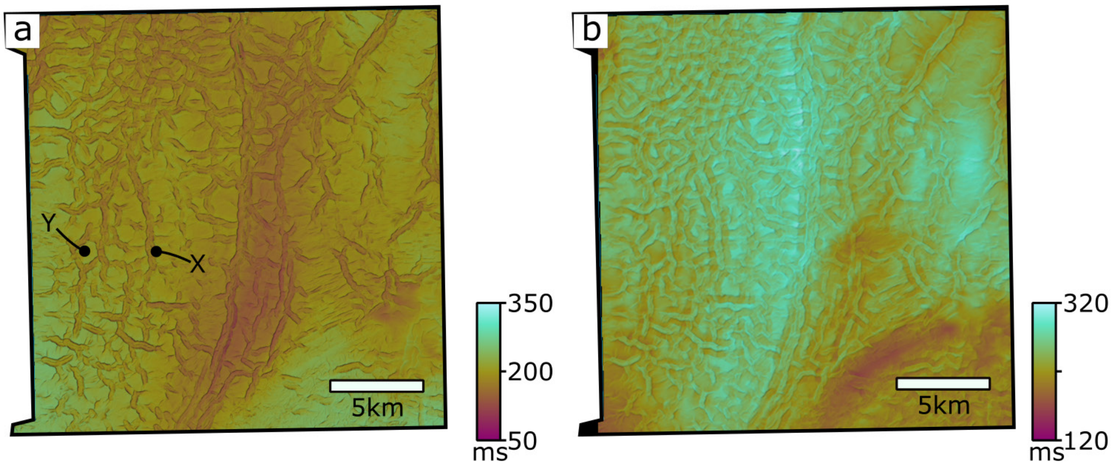

Fig. 6. Isochron maps of (a) K60 to T10 and (b) T10 to T27. On (a), Y indicates the position of a polygonal horst surrounded by a network of narrow grabens. X indicates an elongate trend of narrow grabens, where the underlying tectonic faults have influenced the polygonal fault pattern. See Fig. 2 for location.

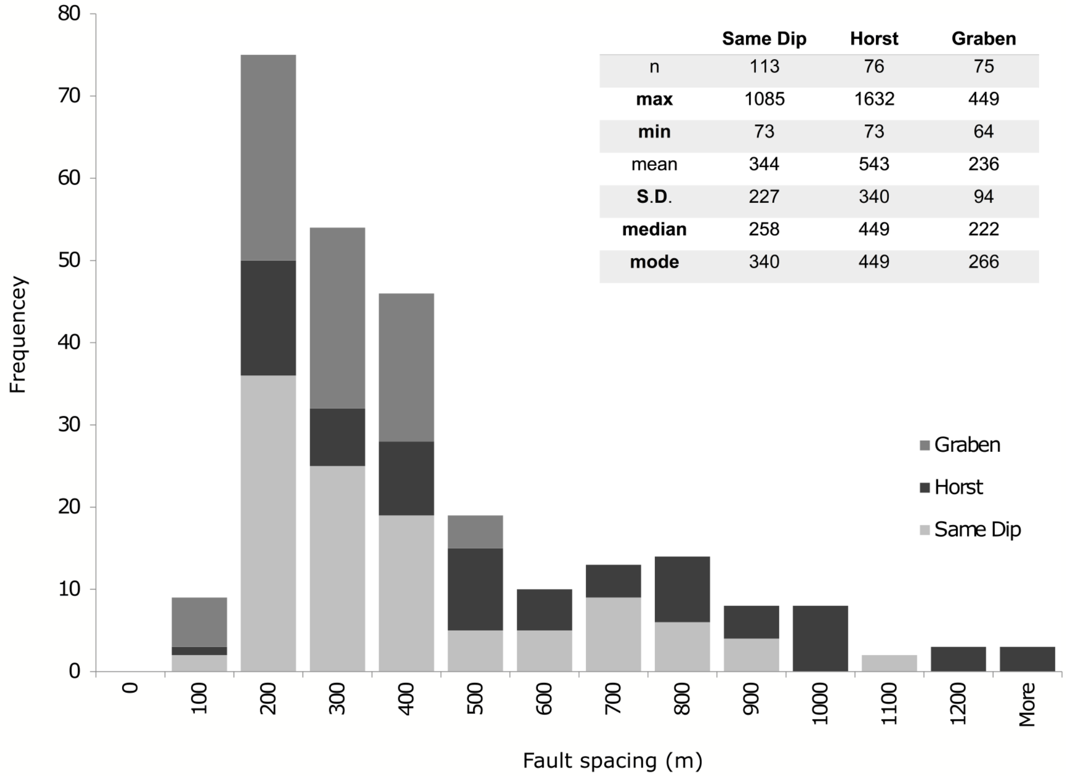

Fig. 7. Histogram illustrating the frequency of faults and fault segments for horsts, grabens and same dip direction segments. The inset table summarizes the statistics for the individual fault populations.

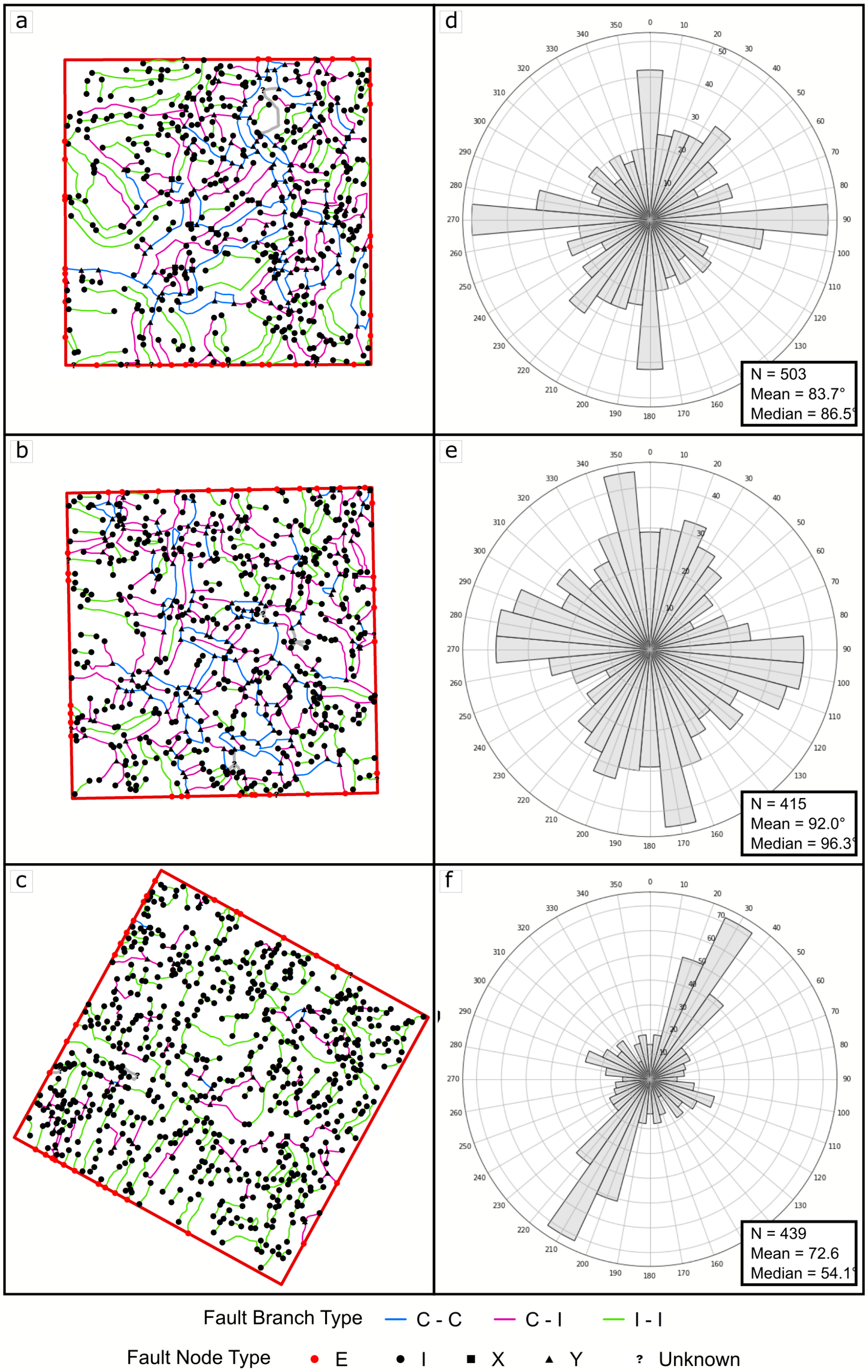

Fig. 8. Fault topology and orientation data for areas A, B and C shown on Fig. 2.

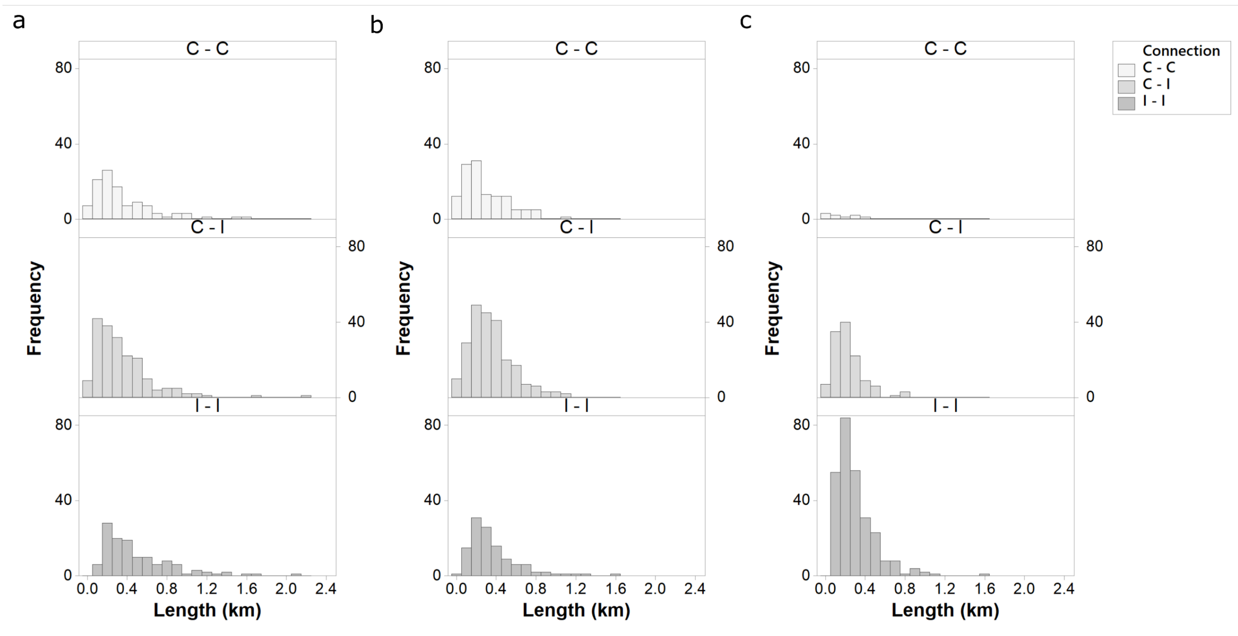

Fig. 9. Fault length for areas (a) A, (b) B and (c) C shown on Fig. 2.